JOURNAL OF Materials CHEMISTRY

Powder diffraction and inelastic neutron scattering studies of the Na_2RbC_{60} fulleride

Kosmas Prassides,*[a] Craig M. Brown,[a,b] Serena Margadonna,[a] Konstantinos Kordatos,[a] Katsumi Tanigaki,[b] Emmanuelle Suard,[b] A. José Dianoux[b] and Kenneth D. Knudsen[d]

[a]*School of Chemistry, Physics and Environmental Science, University of Sussex, Brighton, UK BN1 9QJ*
[b]*Institute Laue-Langevin, F-38042 Grenoble, France*
[c]*Faculty of Science, Osaka-city University, PREST, JST, 3-3-138 Sugimoto, Sumiyoshi-ku, Osaka, 558-8585, Japan*
[d]*European Synchrotron Radiation Facility, F-38043 Grenoble, France*

Received 14th January 2000, Accepted 7th March 2000
Published on the Web 11th May 2000

Neutron and synchrotron X-ray powder diffraction and inelastic neutron scattering (INS) studies of Na_2RbC_{60} in both its polymeric and monomeric phases have been performed as a function of temperature, with particular attention paid to the cooling protocol. The powder diffraction measurements on cooling confirm the slow transformation of the primitive cubic high temperature phase to the monoclinic low temperature phase in the vicinity of 250 K. Rietveld refinements of both the X-ray and neutron data show that over half of the sample transforms to the polymer in the temperature range 180–200 K, this fraction rising to 64(2)% at base temperature. On heating, the percentage of the monomer phase increased from 230 K at the expense of the polymer, with a full transformation occurring by 277 K. A final phase transition to the disordered fcc structure occurs over a range of temperatures from 299 to 317 K. Study of the time evolution of the monomer→polymer transformation at 180 and 200 K allowed us to extract an estimate of the activation barrier to interball C–C bond formation as 0.16(2) eV, comparable to the magnitude of the reorientational potential in the precursor monomer phase. INS spectra in the temperature range 100 to 320 K confirm the reduction of symmetry from the primitive cubic phase through splittings of the intramolecular vibrational modes. The polymeric nature of interfullerene bonding in Na_2RbC_{60} is also confirmed *via* direct observation of excess scattered intensity in the 8–25 meV region of the generalised phonon density-of-states (GDOS).

I Introduction

The study of superconductivity in alkali fullerides with composition $A_2A'C_{60}$ (A, A′ = Na, K, Rb, Cs)[1] has been vigorously pursued. These systems invariably adopt cubic structures and their superconducting transition temperatures, T_c, increase monotonically with increasing lattice constant, a. For large cations (K^+, Rb^+) occupying the tetrahedral interstices, the structures are face-centred-cubic (fcc) (space group $Fm\bar{3}m$)[2] and contain merohedrally disordered C_{60}^{3-} ions. A second structural family is encountered when Na^+ ions reside in the tetrahedral interstices; the crystal structure now changes from fcc at high temperatures to primitive cubic (space group $Pa\bar{3}$)[3–6] near 300 K, as the spherically disordered C_{60}^{3-} ions order orientationally. Evidently the primitive cubic family exhibits a much steeper dependence of the rate of change of T_c with interfullerene separation than that observed for the fcc systems.[3,7]

Even though no superconductivity has been encountered for other alkali fulleride compositions, a genus of the fulleride family with composition AC_{60} (A = K, Rb, Cs) has also attracted considerable interest, principally because of the variety of structural forms encountered. Besides the formation of metastable cubic[8] and dimer[9] structures formed by quenching to low temperatures, direct C–C bonding between the C_{60}^- ions leads to polymer chain formation.[10] The resulting materials adopt quasi-one-dimensional orthorhombic or monoclinic structures (space group *Pmnn* and *I*2/*m*), with the shortest center-to-center interfullerene distance of the order of 9.10 Å, consistent with the formation of *two* C–C bridging bonds.[11] For a while, it seemed that formation of bridged fulleride ions was confined to C_{60}^- and $C_{59}N$[12] units which contain a single unpaired electron in the lowest unoccupied molecular orbital (LUMO). However, recent work on sodium fullerides has led to the realisation that such systems are much more abundant than hitherto appreciated,[13] as polymeric systems containing the C_{60}^{3-} and C_{60}^{4-} ions were synthesised and structurally characterised. For instance, Na_2RbC_{60}, whose ground state structure was thought for a long time to be primitive cubic,[4] was found to form, upon slow cooling, a metallic monoclinic polymeric structure (space group $P2_1/a$, $a = 13.71$, $b = 14.55$, $c = 9.37$ Å and $\beta = 133.53°$) distinctly different from that of the AC_{60} salts, with the short interfullerene distance along c implying the formation of a single C–C bridging bond.[14–18] Such a structure has also been found to form for other sodium and lithium salts, including the $Na_2Rb_{1-x}Cs_xC_{60}$ quaternaries at ambient and elevated pressure[19] and Na_2CsC_{60} and Li_3CsC_{60} at elevated pressure.[20,21] On the other hand, Na_4C_{60} gives rise to a two-dimensional polymer in which the interfulleride bonding is of single C–C bond order between four C_{60}^{4-} nearest neighbours.[22]

In this paper, we present a comprehensive study of the structural and vibrational properties of the Na_2RbC_{60} salt using a combination of experimental techniques. Powder synchrotron X-ray and neutron diffraction were employed to study in detail the monomer to polymer transformation, both as a function of temperature and time. Neutron inelastic scattering measurements were used to characterise both the intramolecular vibrational spectrum of C_{60}^{3-} and to provide direct spectroscopic identification of the interfullerene C–C bridging modes in the intermolecular energy region.

DOI: 10.1039/b000418i

II Experimental

Na_2RbC_{60} was prepared by reaction of stoichiometric quantities of C_{60}, Na and Rb, contained in a sealed Ta cell inside a sealed glass tube filled with He to 500 Torr, at 480 K for 3 h, 570 K for 12 h, and 620 K for 72 h; after an intermediate regrinding, the sample was annealed at 673 K for 25 days. The sample was characterised by solid state NMR, X-ray powder diffraction and SQUID magnetometry.

Neutron powder diffraction measurements on Na_2RbC_{60} (mass = 1.2 g) were performed with the high-flux medium resolution powder diffractometer, D1b, at the Institute Laue-Langevin (ILL), Grenoble, France. The sample was placed in a cylindrical 4 mm diameter vanadium sample holder and was press-sealed with In wire. Data were collected at 5 min intervals throughout the experiment ($\lambda = 2.5242$ Å, $2\theta = 10$–$90°$). The applied heat treatment protocol comprised of cooling from 315 to 180 K at a rate of 5 K h^{-1}, remaining at 180 K for 12 h, and then cooling to 2 K at 72 K h^{-1}. Following optimisation of the diffracted intensity that provided a doubling of the observed counting rate, the sample was then heated from 2 to 350 K at a rate of 16.5 K h^{-1}.

Synchrotron X-ray powder diffraction measurements were performed on the Na_2RbC_{60} sample sealed in a thin-wall glass capillary 0.5 mm in diameter between 320 and 200 K. The sample was first cooled at 30 K h^{-1} to 200 K, where it was kept for 7 h. It was then heated to 310 K at the same rate. Images of the Debye–Scherrer rings were recorded on the 300 mm diameter Mar Research circular image plate system on line A of the BM1 beamline at the European Synchrotron Radiation Facility, Grenoble. A monochromatic X-ray beam of wavelength $\lambda = 0.8736$ Å and dimensions 0.5×0.5 mm^2 was focussed onto the sample by sagittal bending of the second crystal of the double-crystal Si(111) monochromator together with a vertically focussing Rh-coated Zerodur mirror. Patterns were measured with sample-to-detector distances of 200, 300 and 420 mm for periods of 180 s. During the data collection the sample was rotated about its axis by 30°. Cooling was by means of an Oxford Cryosystems Cryostream cold nitrogen blower. One-dimensional diffraction patterns were obtained by integrating around the rings using local software (program FIT2D). Prior to integration, the centre of the rings and the tilt angles of the image plate with respect to the incident beam were refined using the 10 strongest rings in the diffraction pattern.

Inelastic neutron scattering measurements on Na_2RbC_{60} (mass = 1.2 g) were performed with both the IN6 spectrometer at the ILL and the time-focused crystal analyzer (TFXA) spectrometer at ISIS, Rutherford Appleton Laboratory, UK. IN6 is a time-focused time-of-flight (TOF) instrument operating in neutron energy gain. An incident neutron wavelength of 4.12 Å was used. The instrumental resolution at this wavelength is 0.1 meV at the elastic line and 3.5 meV at 25 meV energy transfer. The sample was placed inside a thin-wall cylindrical aluminium can (i.d. = 8 mm) and press-sealed with In wire. It was then cooled to 200 K at 8.7 K h^{-1}, where it remained for 24 h before further cooling to 100 K. Data were collected on heating at 100, 200 and 320 K over the full range of scattering angles (10°–115°), and later summed to improve statistics at the expense of momentum resolution. Corrections to the data were made for the aluminium can contribution, detector efficiency and geometry. TFXA is an inverted geometry instrument, operating at a fixed neutron final energy of $E_f = 4$ meV and with incident energy analysis performed by TOF. Time and energy focusing gives excellent resolution, $(\delta\omega/\omega) \approx 1$–2% over a wide range of energies. A similar cooling protocol was followed for the TFXA experiment and the sample was cooled from room temperature to 180 K at a rate of 4.8 K h^{-1}, followed by cooling to 6 K at 7 K h^{-1}. The sample had been press-sealed using In wire inside a 6 mm i.d. vanadium can and data were collected at 6 K over a total incident current of ~10 mA (at a rate of ~180 μA h^{-1}). A dataset of the empty vanadium can was also collected at 6 K and was subtracted from the data.

To allow direct comparisons to the scattering law, $S(Q,\omega)$, at base temperature, the IN6 spectra were normalised by the Bose occupation factors, such that the normalised $S(Q,\omega)_n$ is given by

$$S(Q,\omega)_n = S(Q,\omega)\ \frac{n(\omega)_0}{n(\omega)_T} \tag{1}$$

where $n(\omega) = (e^{-\beta} - 1)^{-1}$ and the subscripts 0 and T refer to base temperature and the actual temperature at which the spectrum was collected, respectively.

Within the framework of the incoherent approximation,[23] the spectral distribution function $P(\bar{\alpha},\beta)$ is given by

$$P(\bar{\alpha},\beta) = 2\beta\ \sinh\left(\frac{\beta}{2}\right)\ \left(\frac{S(Q,\omega)}{\bar{\alpha}}\right) \tag{2}$$

where $S(Q,\omega)$ is the uncorrected symmetrized scattering law and the dimensionless variables $\bar{\alpha}$ and β are related to momentum and energy transfer, respectively through

$$\bar{\alpha} = \frac{\hbar^2 Q^2}{2MkT};\quad \beta = \frac{\hbar\omega}{kT} \tag{3}$$

where M is an average atomic mass. The spectral distribution function $P(\bar{\alpha},\beta)$ can be corrected for instrumental background, Debye–Waller and multiphonon contributions, using approximate analytic procedures in a self-consistent manner.[24] This results in a corrected one-phonon spectral distribution function, $P_1(\bar{\alpha},\beta)$ from which the generalized or 'neutron-weighted' phonon DOS, $G(\omega)$ is obtained:

$$G(\omega) = \exp(2W) P_1(\bar{\alpha},\beta) \tag{4}$$

where $\exp(-2W)$ is the Debye–Waller attenuation factor. For polyatomic compounds, like the present fulleride salts, $G(\omega)$ is related to the partial phonon DOS, $g_i(\omega)$, for each atom i through the expression

$$G(\omega) = \left[\sum_i \left(\frac{c_i\sigma_i}{m_i}\right)\right]^{-1} \sum_i \left(\frac{c_i\sigma_i}{m_i}\right) g_i(\omega) \tag{5}$$

where σ_i is the total neutron scattering cross section for atom i, m_i its mass and c_i its concentration ($\Sigma_i c_i = 1$).

Finally, for small fixed final energy instruments like TFXA, $G(\omega)$ is given by:

$$G(\omega) = \frac{S(Q,\omega) 2m\omega}{\hbar^2 Q^2 [n(\omega) + 1]} \tag{6}$$

with the ratio (Q^2/ω) being essentially constant, resulting in a scattering law that is directly proportional to the generalised phonon DOS.

III Results and discussion

A Neutron diffraction results

Fig. 1 shows the evolution of the neutron diffraction profiles of Na_2RbC_{60} between 150 and 350 K in the 2θ range 28–39°, as obtained on heating with the D1b diffractometer. The intensity is displayed in a logarithmic fashion in order to aid visualisation of the phase transitions which occur in this temperature range. At low temperatures, the patterns are dominated by low-intensity broad peaks. There is a drastic change in the profiles in the vicinity of 270–280 K, whence many peaks disappear while others gain significantly in intensity. These changes correspond well to the established structural behaviour of Na_2RbC_{60}, namely that a transition from a monoclinic to a primitive cubic structure occurs at these

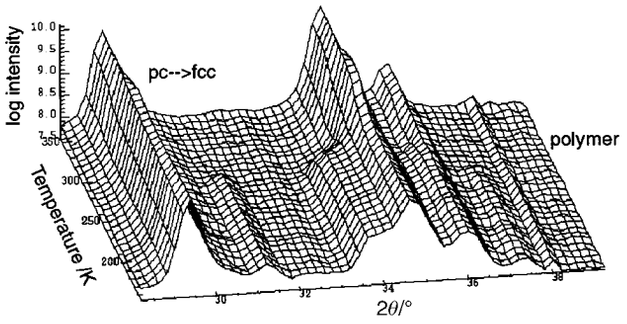

Fig. 1 Temperature dependence of a selected region ($2\theta = 28$–$39°$) of the powder neutron diffraction profile of Na_2RbC_{60} measured on D1b on heating. The polymer→monomer transformation is evident by the changes in the profile at ~ 280 K, while the primitive cubic→fcc transition is reflected in the *d*-spacing shift at around 300 K. Note the use of a logarithmic intensity scale.

temperatures.[14,16] Shortly after this, a second transformation occurs to a fcc phase at ~ 299 K; this is accompanied by a shift in the position of the cubic peaks to lower 2θ, in agreement with the discontinuous lattice expansion at the transition temperature.

The data were analysed in the temperature range 2–350 K by both single-phase and two-phase sequential Rietveld profile analysis, using the program FULLPROF[25] and employing the published structures for the monomer[3] and polymer[16,17] forms of Na_2RbC_{60}. The polymer structure is monoclinic (space group $P2_1/a$) and derives from that of the primitive cubic structure, after a contraction along one of the cubic face diagonals and a tilt of one of the axes. The C_{60}^{3-} ions are linked by single C–C bonds (~ 1.7 Å), which lie on the *bc* plane and are inclined to the *c* axis by $\sim 7.7°$ (Fig. 2). The alkali metals reside in the (0.5,0,0) and (0,0.25,0.5) positions, derived from the high symmetry tetrahedral and octahedral sites of the parent structure.

The results of two-phase (coexisting monoclinic and cubic phases) Rietveld refinement at 2.3 K are shown in Fig. 3 ($R_{wp} = 5.0\%$, $R_{exp} = 1.8\%$). The refined lattice parameters are $a = 13.66(1)$, $b = 14.420(8)$, $c = 9.354(6)$ Å and $\beta = 133.57(6)°$ for the polymer and $a = 13.99(1)$ Å for the monomer phase, respectively, while the fraction of the polymer phase is 64(2)%. The temperature evolution of the lattice parameters for all phases, obtained on heating, are shown in Fig. 4. The strong anisotropic bonding present in the polymer phase is clearly evidenced by the negligible thermal expansivity, $\alpha_c = -4(5) \times 10^{-7}$ K^{-1} in the temperature range 100 to 230 K

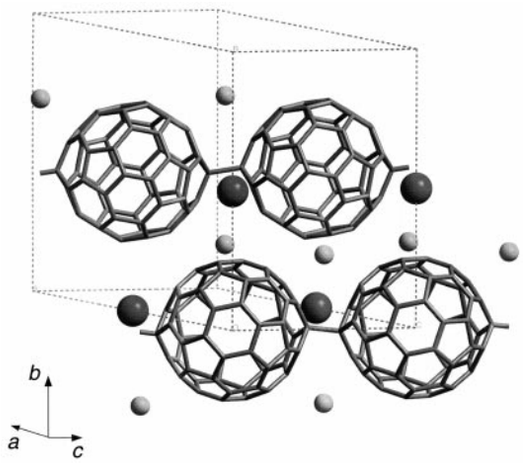

Fig. 2 Crystal structure of the Na_2RbC_{60} polymer. The polymer chains are aligned along the *c* axis of the cell with the fullerenes connected by single C–C bonds. Na^+ and Rb^+ ions are shown as small and large spheres, respectively.

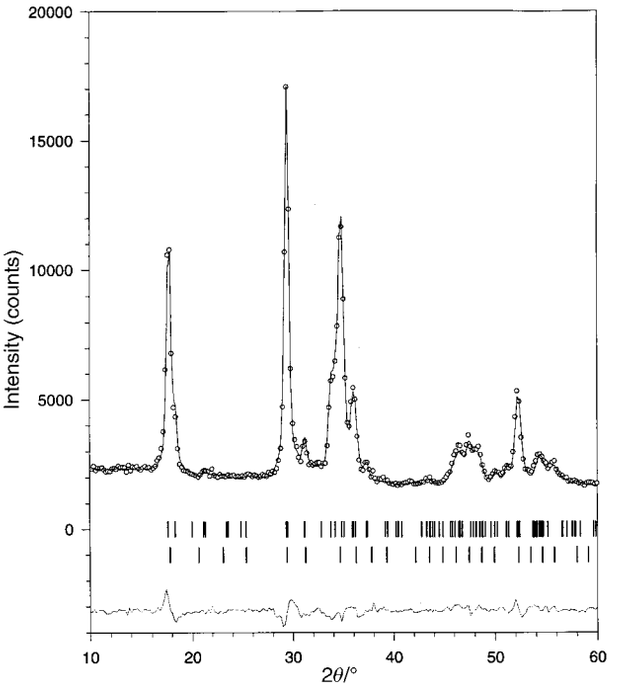

Fig. 3 Final observed (open circle) and calculated (solid line) neutron ($\lambda = 2.5242$ Å) powder diffraction profile of Na_2RbC_{60} at 2.3 K after slow cooling. The lower line shows the difference profile and the vertical marks indicate the predicted reflections (monoclinic phase = top, cubic phase = bottom set).

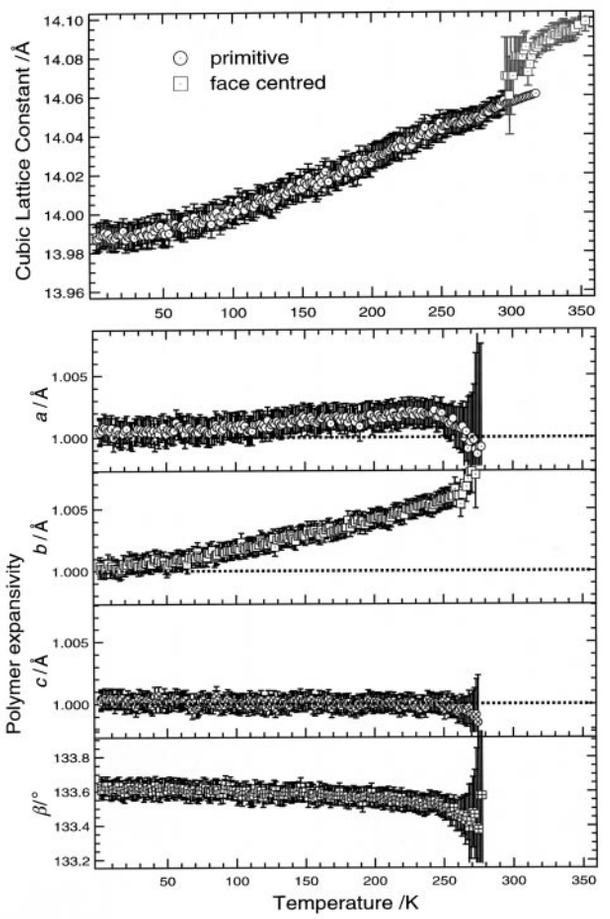

Fig. 4 Temperature evolution of the lattice constant of cubic Na_2RbC_{60} (upper panel) and the normalized lattice parameters (to their 2.3 K values) *a*, *b*, *c* and angle β (lower panel) of monoclinic Na_2RbC_{60}, as extracted from the powder neutron diffraction data during heating.

found along the chain axis, c. This is in sharp contrast with the value of the expansitivity along b, $\alpha_b = 2.41(5) \times 10^{-5}\ K^{-1}$, which is comparable to those found in monomeric fulleride phases (*e.g.* in the primitive cubic phase, $\alpha = 1.96(4) \times 10^{-5}\ K^{-1}$). The expansivity of the monoclinic a-axis, $\alpha_a = 8.0(7) \times 10^{-6}\ K^{-1}$ behaves in an intermediate manner, reflecting the steric influence of the Rb^+ ions at the (0.5,0,0) sites.

The temperature dependence of the fraction of the primitive cubic phase during both the cooling and heating cycles is shown in Fig. 5. On heating, the fractions of the monomer and polymer phases remain essentially temperature independent over a wide range of temperatures (2–230 K). Then, the polymer fraction starts decreasing sharply until complete disappearance of the polymer phase has occurs by 277 K. Above 278 K, the data can be described in terms of the primitive cubic structure alone. Transformation to the fcc phase occurs at 299 K, with co-existing primitive cubic and fcc phases[14] present up to 317 K. Above this temperature, satisfactory refinements of the diffraction profiles could be achieved by employing a model of a single fcc component [$a = 14.085(5)$ Å at 317 K and 14.098(5) Å at 353 K]. The data obtained on cooling were not of sufficient quality to allow the precise determination of the transition temperatures, as above 250 K the polymer fraction is small and peak overlap extensive. Despite this, Fig. 5 shows the presence of strong hysteretic behaviour for the formation and destruction of the polymer phase, as at all temperatures down to about 180 K the polymer fraction is larger during the cooling cycle.

Finally, the evolution of the fraction of the polymeric phase, ϕ, was followed during the 12 h equilibration period at 180 K in the course of the slow cooling protocol. ϕ increases over this period by only $\sim$4.4%, with its time dependence described by the equation:

$$\phi(T,t) = \phi(T,0) + \frac{t}{\tau(T)} \qquad (7)$$

where $\phi(180\ K,0) = 0.556(2)$ and $\tau(180\ K) = 1.6(1) \times 10^4$ min. $\tau(T)$ is the structural transformation relaxation time at a temperature T. The extremely slow kinetics of the polymerisation reaction are clearly evident with a complete transformation at this temperature necessitating approximately 120 h.

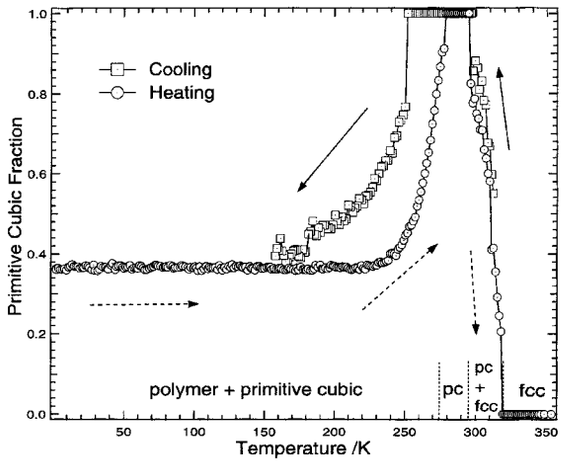

Fig. 5 Temperature evolution of the volume fraction of the primitive cubic phase of Na_2RbC_{60}, as obtained from Rietveld analysis of powder neutron diffraction data during cooling (squares and full arrows) and heating (circles and dashed arrows) cycles. On heating, there are four compositional regions, as indicated: single-phase fcc between 317 and 350 K, primitive cubic and fcc coexistence between 296 and 317 K, single-phase primitive cubic between 278–296 K, and monoclinic and primitive cubic coexistence below 278 K.

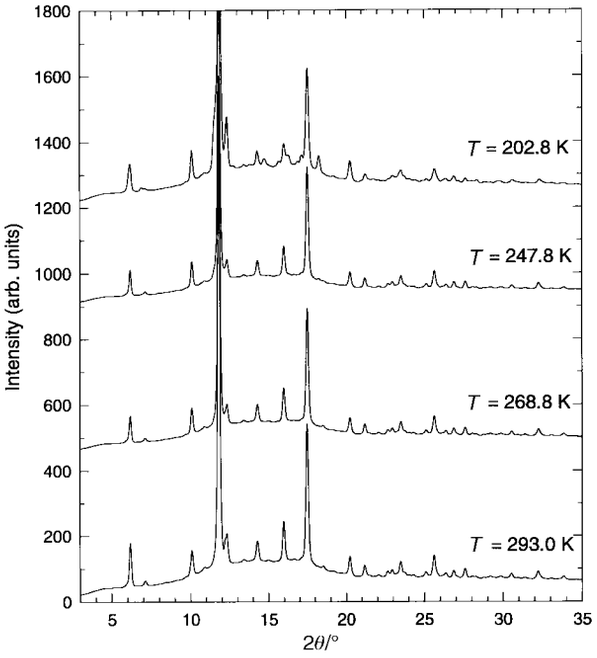

Fig. 6 Temperature variation of the powder synchrotron X-ray diffraction profiles of Na_2RbC_{60} ($\lambda = 0.873$ Å) on slow cooling.

B Synchrotron X-ray diffraction results

Temperature-dependent synchrotron X-ray powder diffraction was also used to study the monomer→polymer transition in Na_2RbC_{60} during both slow cooling and heating protocols (Fig. 6). In agreement with the neutron diffraction results, the fraction of the polymeric phase starts to become significant on cooling at a temperature of $\sim$250 K ($\phi \approx 0.10$) and increases monotonically to $\phi \approx 0.53$ as the temperature approaches 200 K (Fig. 7). The transformation continues to take place slowly as the sample temperature is kept at 200 K. After an equilibration period of 7 h at 200 K, ϕ has only increased by $\sim$0.07 (Fig. 8). Its time evolution can be again approximately described by eqn. (7) with $\phi(200\ K,0) = 0.530(2)$ and $\tau(200\ K) = 5.6(3) \times 10^3$ min. The extremely slow kinetics are again clearly evident and a complete transformation of the cubic to the polymer phase at 200 K would require $\sim$44 h, approximately one third of the time needed previously at 180 K. The extracted values of the relaxation times, τ, at 180 and 200 K can be used to obtain an estimate of the activation barrier for polymer formation. Assuming that τ exhibits a simple activated behaviour:

$$\tau(T) = \frac{1}{\nu_0} \exp\left(\frac{E_a}{kT}\right) \qquad (8)$$

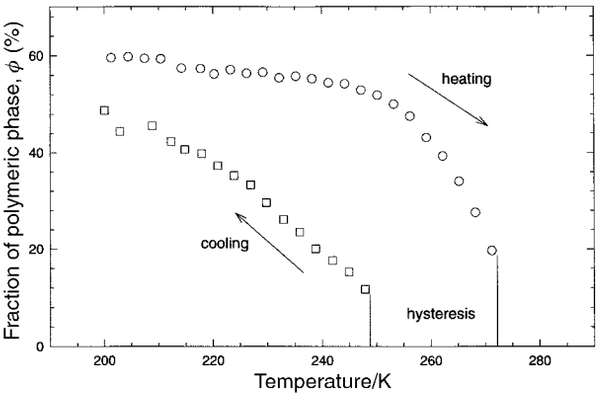

Fig. 7 Temperature evolution of the volume fraction of the monoclinic phase of Na_2RbC_{60}, as obtained from Rietveld analysis of synchrotron X-ray powder diffraction data during cooling and heating cycles.

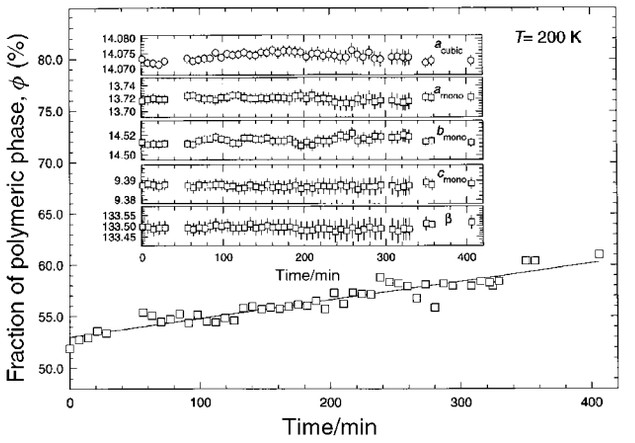

Fig. 8 Time evolution of the polymer phase fraction of Na_2RbC_{60} at 200 K. The line represents a linear fit of the data. Inset: time evolution of the lattice constants at 200 K.

with $1/v_0$ describing an attempt frequency, the activation energy, E_a is obtained as 0.16(2) eV, comparable to that of the cubic→polymer transformation in KC_{60} [$E_a = 0.17(5)$ eV][26] and to the rotational barrier for C_{60} reorientations in primitive cubic Na_2RbC_{60}.[6] This is consistent with a mechanism for C–C formation in polymeric Na_2RbC_{60} in which small-amplitude orientational jumps are required to achieve optimal contact between fullerene neighbouring molecules in the precursor primitive cubic phase for polymerisation to occur. Finally, on heating, strong hysteretic behaviour is again observed, with the monoclinic phase now disappearing at $\approx$270 K (Fig. 7).

C Inelastic neutron scattering results

Fig. 9 shows the inelastic neutron scattering spectrum of Na_2RbC_{60} measured on TFXA between 2 and 200 meV at 6 K. The vibrational spectrum is characterised by fundamental modes in the intermolecular vibrational energy region from 2 to 30 meV, as well as in the intramolecular region above 30 meV. In the intramolecular region, there are modes at 4.1(2), 12.6(1) and 16.9(4) meV. Both theoretical calculations[27] and experimental studies of the vibrational spectrum of C_{60}[28] have shown that the intermolecular vibrations in pristine monomeric C_{60} are soft and appear at energies below 8 meV, while the Rb^+–C_{60}^{3-} and Na^+–C_{60}^{3-} modes are expected below 15–20 meV.[29] At the same time, in polymeric fullerides in which there are covalent bridging bonds between the fullerene units, interball C–C vibrations should also appear in the low-energy part of the vibrational spectrum. Theoretical calculations based on a first-principles quantum molecular dynamics model of polymerised fullerenes[30] place the interball C–C vibrations in the 10–20 meV energy region, in agreement with experimental results on C_{60} and AC_{60} (A = Rb, Cs) polymers.[31,32] Based on the above observations, we can rationalise the intermolecular part of the vibrational spectrum of polymer Na_2RbC_{60}. The mode at 4.1(2) meV can be assigned to interfullerene and to alkali metal–fullerene interactions, while the modes at 12.6(1) and 16.9(4) meV are due to the intermolecular C–C vibrations along the polymer chain (*vide infra*). The latter overlap with the Na^+–fullerene vibrations, which are also expected in the same energy range.

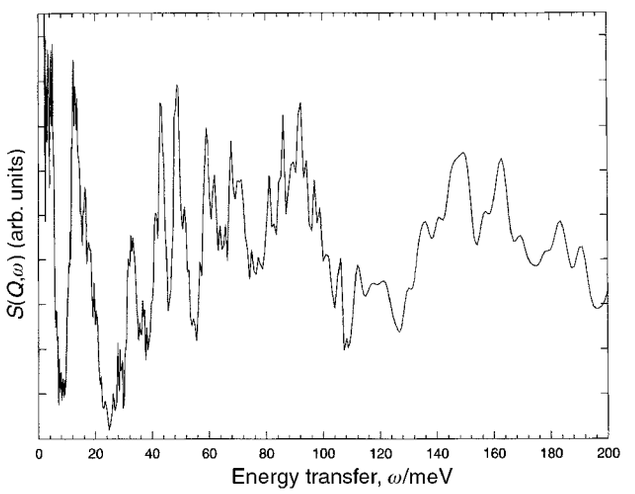

Fig. 9 Inelastic neutron scattering spectrum of Na_2RbC_{60} in the energy region 2–200 meV at 6 K.

Above 30 meV, many well defined peaks of the polymer are present (Fig. 9). Their energies are in good agreement with those of C_{60} and AC_{60} polymers. This intramolecular vibrational region can be further subdivided into two parts. The tangential modes are in the high-energy (108–200 meV) and the radial modes in the low-energy (30–108 meV) region. A tentative assignment of some of the radial modes can be made by reference to pristine C_{60} and K_3C_{60}.[28,33] There are well-resolved bands at 28.5(2), 33.01(9) ($H_g^{(1)}$), 41.46(8), 43.35(7) (T_{2u}, G_u), 48.78(9), 51.682) (H_u, $H_g^{(2)}$), 59.1(1) (G_g), 67.69(4), 85.9(2), and 97.3(4) meV. It is noteworthy that the $H_g^{(1)}$ mode at 33 meV remains unsplit in the Na_2RbC_{60} polymer, reminiscent of the situation in the singly bonded AC_{60} dimeric phases[31] and in contrast to the well-resolved splittings observed for doubly bonded AC_{60} polymers. In the high-energy region, there are no sharp well-defined features. When compared to C_{60}, there is a general softening of the vibrational modes throughout the spectrum.

The scattering law, $S(Q,\omega)$, of Na_2RbC_{60} was also measured at an average $Q = 1.47$ Å^{-1} at 100, 200 and 320 K with the IN6 spectrometer. The data were corrected for contributions from the empty can, normalised to vanadium and then summed over all scattering angles, except for those contaminated by elastic Bragg peaks. The data after normalisation by the Bose occupation factor according to eqn. (1) are displayed in Fig. 10. At both 100 and 200 K when the polymer and cubic phases coexist, there are two excitations evident in the measured spectra. These can be adequately described by fitting with two Gaussian peaks, convoluted with the instrumental resolution function. At 200 K, these are located at 3.30(5) and 2.92(8) meV with full widths at half maximum (FWHM) of 3.08(8) and 0.4(1) meV, respectively. Similar features are present in the low-energy inelastic spectra of the doubly bridged AC_{60} (A = Rb, Cs) polymers[31,34,35] and have been assigned to twisting modes of the polymer chains. At 320 K, when the polymer phase has disappeared, quasielastic scattering also appears. This can be well described by a broad Lorentzian line, centred at zero-energy transfer, of FWHM = 4.8(1) meV and implying the existence of diffusive rotational motion in the high temperature orientationally disordered fcc phase of Na_2RbC_{60}.[6,36]

The generalized phonon density-of-states, $G(\omega)$, was extracted from the full angular range of the data, as described in Section II, and is shown in Fig. 11 for the energy range 0–38 meV at temperatures of 200 and 320 K. In the energy transfer window shown, there are four features of note at both 200 and 320 K: three peaks at $\sim$4, 7 and 34 meV that remain almost unchanged by the transformation to the cubic phase and a broad peak between 8 and 25 meV that is strongly suppressed in intensity on going through the polymer→monomer transition. In order to exemplify this situation further, the bottom panel of Fig. 11 shows the difference curve obtained by subtracting the high temperature (cubic monomer phase) from the low temperature (two-phase mixture of polymer and monomer phases) data. The only feature which survives this subtraction is the broad peak at 8–25 meV which coincides with the intermolecular region of the vibrational spectra of

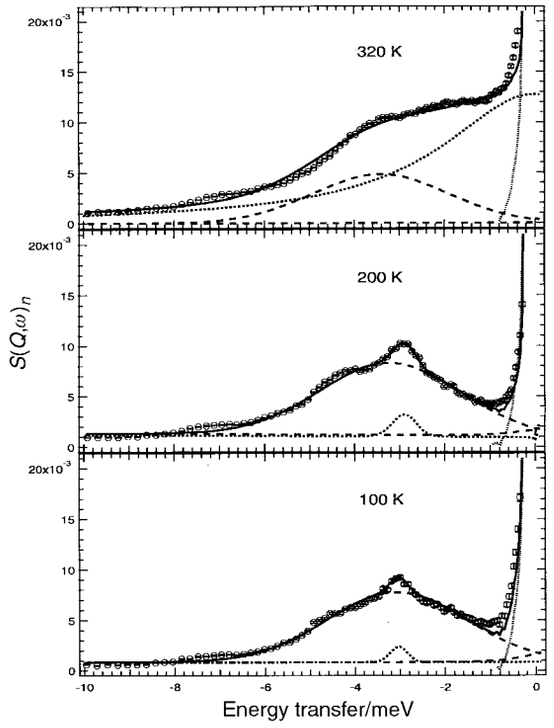

Fig. 10 Near inelastic neutron scattering spectra ($Q_{av}=1.4$ Å^{-1}) of Na_2RbC_{60} at 100, 200 and 320 K. The data at 200 and 320 K are scaled by the Bose factor. Each panel shows the normalised scattering law, $S(Q,\omega)_n$ (open circles) and the fitted spectra (solid lines) to one Gaussian and one Lorentzian (320 K) or two Gaussian (100 and 200 K) components (broken lines), convoluted with the resolution function. A delta function is also included at the elastic line in each case.

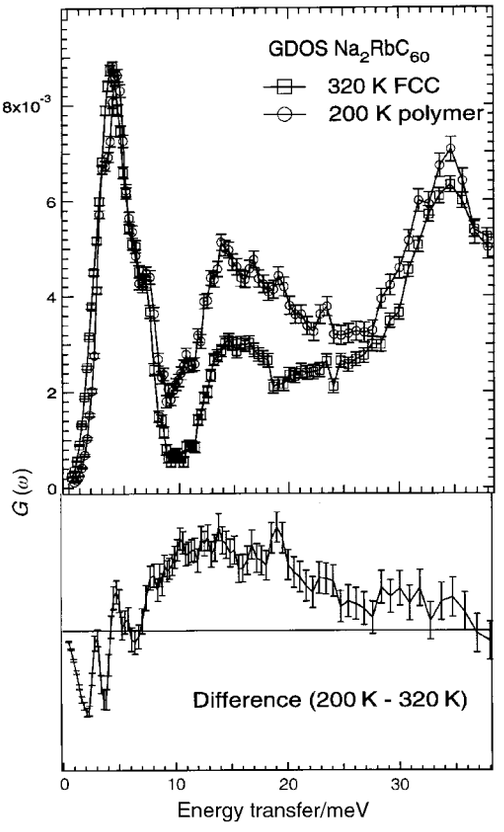

Fig. 11 Upper panel: low-energy part of the generalised phonon density-of-states (GDOS) for Na_2RbC_{60} at 320 (squares) and 200 K (circles). Lower panel: difference between the two PDOS curves, showing the existence of phonon modes in the energy range 8–25 meV that arise from the bridging C–C bonds in the polymer phase.

fullerenes and their derivatives. The lowest lying modes are assigned to C_{60}^{3-} translational and librational modes and to Rb^+ optic modes, while the highest energy mode at 34 meV is assigned to the lowest energy intramolecular mode, $H_g^{(1)}$ of C_{60}^{3-}, as also detailed earlier for the TFXA data. A closer look at this shows an asymmetry and discernible kinks—a manifestation of the lowering in symmetry in the polymer phase. The details of the intermolecular modes differ from those seen in polymeric RbC_{60}, implying somewhat different van der Waals parameters for these bonds.[29] The overwhelming feature, however, is the reduction in scattering intensity in the 8–25 meV region on heating to 320 K. Both the spectra at 200 and 320 K contain a substantial peak at ~15 meV that is due to sodium optic modes and so a direct subtraction of the two spectra gives the excess scattering associated with the polymer phase, shown in the lower panel of Fig. 11. While the error bars are quite large, a distinct maximum in the scattering is found between 8 and 18 meV, providing strong evidence for the polymeric nature and the presence of interfullerene bridging C–C bonds in the low temperature phase. This can be compared to the scattering found in the RbC_{60} polymer (broad intensity distribution between 12 and 23 meV) and dimer (three sharp peaks at 10.4, 12.2 and 13 meV) phases.[31] Even though the broad distribution of intensity of the doubly bonded polymer remains, we also see a significant softening on going from RbC_{60} to Na_2RbC_{60} of approximately 5 meV. This is indicative of weaker interfullerene bonding, which is consistent with the singly bonded nature of the Na_2RbC_{60} polymer.

IV Conclusions

Powder neutron and synchrotron X-ray diffraction measurements have been used to characterise the thermal evolution of the monomer→polymer phase transition in Na_2RbC_{60}. The transformation occurs at ~250 K on cooling and never goes to completion. The rate of polymer formation is very slow and temperature dependent. Upon heating from 2.3 K, the weight fraction of the polymer remains constant up to 230 K, when the fraction of the primitive cubic phase begins to increase. Strong hysteresis effects are observed with the polymer now surviving up to 277 K. The thermal evolution of the monoclinic lattice constants is characterised by strong anisotropy, consistent with the anisotropic bonding present. Negligible expansitivity is observed along the c axis that defines the polymer chain direction. Detailed time-dependent measurements of the powder diffraction profiles at 180 and 200 K allowed us to extract the relaxation times for the formation of the polymer at these temperatures. These in turn led to an estimate of the activation energy for polymerisation, $E_a=0.16(2)$ eV, which is of the same order of magnitude as the rotational activation barrier in primitive cubic Na_2RbC_{60}.

Inelastic neutron scattering measurements of slowly cooled Na_2RbC_{60} showed excess scattering appearing on cooling through the monomer→polymer transition in the 8–25 meV energy region. This broad vibrational DOS is located at slightly reduced energies compared with those observed for the doubly bridged AC_{60} polymers, consistent with the formation of a single C–C bond between fullerene units. The librational spectrum of the polymer also shows a broad distribution of modes centred at ~3.5 meV that are assigned to twisting motions of the polymer chains about their axis. At high temperatures, the spectrum is characterised by the presence of a quasielastic peak, signature of rotational diffuse motion of the C_{60}^{3-} ions in the orientationally disordered fcc phase.

Acknowledgements

We thank the NEDO FCT program for financial support, the ILL and Rutherford Appleton Laboratory for provision of neutron and the ESRF for provision of synchrotron X-ray beamtime. We thank Dr Stewart Parker for help with the TFXA experiment and Dr Helmut Schober for the use of his sample holder in the IN6 measurements.

References

1 O. Gunnarsson, *Rev. Mod. Phys.*, 1997, **69**, 575; M. J. Rosseinsky, *Chem. Mater.*, 1998, **10**, 2665.
2 P. W. Stephens, L. Mihaly, P. L. Lee, R. L. Whetten, S. M. Huang, R. Kaner, F. Deiderich and K. Holczer, *Nature*, 1991, **351**, 632.
3 K. Prassides, C. Christides, I. M. Thomas, J. Mizuki, K. Tanigaki, I. Hirosawa and T. W. Ebbesen, *Science*, 1994, **263**, 950.
4 K. Kniaz, J. E. Fischer, Q. Zhu, M. J. Rosseinsky, O. Zhou and D. W. Murphy, *Solid State Commun.*, 1993, **88**, 47.
5 K. Tanigaki, I. Hirosawa, T. Manako, J. S. Tsai, J. Mizuki and T. W. Ebbesen, *Phys. Rev. B*, 1994, **49**, 12307.
6 C. Christides, K. Prassides, D. A. Neumann, J. R. D. Copley, J. Mizuki, K. Tanigaki, I. Hirosawa and T. W. Ebbesen, *Europhys. Lett.*, 1993, **24**, 755.
7 T. Yildirim, J. E. Fischer, R. Dinnebier, P. W. Stephens and C. L. Lins, *Solid State Commun.*, 1995, **93**, 269.
8 A. Lappas, M. Kosaka, K. Tanigaki and K. Prassides, *J. Am. Chem. Soc.*, 1995, **117**, 7560.
9 Q. Zhu, D. E. Cox and J. E. Fischer, *Phys. Rev. B*, 1995, **51**, 3966; G. Oszlanyi, G. Bortel, G. Faigel, M. Tegze, L. Granasy, S. Pekker, P. W. Stephens, G. Bendele, R. Dinnebier, G. Mihaly, A. Janossy, O. Chauvet and L. Forro, *Phys. Rev. B*, 1995, **51**, 12228.
10 P. W. Stephens, G. Bortel, G. Faigel, M. Tegze, A. Janossy, S. Pekker, G. Oszlanyi and L. Forro, *Nature*, 1994, **370**, 636.
11 P. Launois, R. Moret, J. Hone and A. Zettl, *Phys. Rev. Lett.*, 1998, **81**, 4420.
12 J. C. Hummelen, B. Knight, J. Pavlovich and R. Gonzalez, *Science*, 1995, **269**, 1554; C. M. Brown, L. Cristofolini, K. Kordatos, K. Prassides, C. Bellavia, R. Gonzalez, K. M. Keshavarz, F. Wudl, A. K. Cheetham, J. P. Zhang, W. Andreoni, A. Curioni, A. N. Fitch and P. Pattison, *Chem. Mater.*, 1996, **8**, 2548.
13 K. Prassides, *Curr. Opin. Solid State Mater. Sci.*, 1997, **2**, 433.
14 K. Prassides, K. Vavekis, K. Kordatos, K. Tanigaki, G. M. Bendele and P. W. Stephens, *J. Am. Chem. Soc.*, 1997, **119**, 834.
15 L. Cristofolini, K. Kordatos, G. A. Lawless, K. Prassides, K. Tanigaki and M. P. Waugh, *Chem. Commun.*, 1997, 375.
16 G. M. Bendele, P. W. Stephens, K. Prassides, K. Vavekis, K. Kordatos and K. Tanigaki, *Phys. Rev. Lett.*, 1998, **80**, 736.
17 A. Lappas, C. M. Brown, K. Kordatos, E. Suard, K. Tanigaki and K. Prassides, *J. Phys.: Condens. Matter*, 1999, **11**, 371.
18 D. Arcon, K. Prassides, S. Margadonna, A. L. Maniero, L. C. Brunel and K. Tanigaki, *Phys. Rev. B*, 1999, **60**, 3856.
19 K. Prassides, K. Tanigaki and Y. Iwasa, *Physica C*, 1997, **282**, 307.
20 S. Margadonna, C. M. Brown, A. Lappas, K. Prassides, K. Tanigaki, K. D. Knudsen, T. Le Bihan and M. Mezouar, *J. Solid State Chem.*, 1999, **145**, 471.
21 S. Margadonna, K. Prassides, K. D. Knudsen, M. Hanfland, M. Kosaka and K. Tanigaki, *Chem. Mater.*, 1999, **11**, 2960.
22 G. Oszlanyi, G. Baumgartner, G. Faigel and L. Forro, *Phys. Rev. Lett.*, 1997, **78**, 4438.
23 P. A. Egelstaff and P. Shofield, *Nucl. Sci. Eng.*, 1962, **12**, 60.
24 A. J. Dianoux and R. Currat, unpublished work.
25 J. Rodriguez-Carvajal, Program FULLPROF (version 3.5, Dec. 97), ILL, unpublished.
26 J. Robert, P. Petit and J. E. Fischer, *Physica C*, 1996, **262**, 27.
27 F. Negri, G. Orlandi and F. Zerbetto, *Chem. Phys. Lett.*, 1988, **144**, 31; J. Kohanoff, W. Andreoni and M. Parrinello, *Phys. Rev. B*, 1992, **46**, 3671; C. Z .Wang, C. T. Chan and K. M. Ho, *Phys. Rev. B*, 1992, **46**, 9671.
28 K. Prassides, T. J. S. Dennis, J. P. Hare, J. Tomkinson, H. W. Kroto, R. Taylor and D. R. M. Walton, *Chem. Phys. Lett.*, 1991, **187**, 455; C. Coulombeau, H. Jobic, P. Bernier, C. Fabre, D. Schutz and A. Rassat, *J. Phys. Chem.*, 1992, **96**, 22; R. L. Cappelletti, J. R. D. Copley, W. A. Kamitakahara, F. Li, J. S. Lannin and D. Ramage, *Phys. Rev. Lett.*, 1991, **66**, 3261; L. Pintschovius, B. Renker, F. Gompf, R. Heid, S. L. Chaplot, M. Haluska and H. Kuzmany, *Phys. Rev. Lett.*, 1992, **69**, 2662.
29 B. Renker, F. Gompf, H. Schober, P. Adelmann, H. J. Bornemann and R. Heid, *Z. Phys. B*, 1993, **92**, 451; B. Renker, H. Schober and R. Heid, *Appl. Phys. A*, 1997, **64**, 271.
30 G. B. Adams, J. B. Page, O. F. Sankey and M. O'Keeffe, *Phys. Rev. B*, 1994, **50**, 17471.
31 B. Renker, H. Schober, F. Gompf, R. Heid and E. Ressouche, *Phys. Rev. B*, 1996, **53**, 14701.
32 L. Cristofolini, C. M. Brown, A. J. Dianoux, M. Kosaka, K. Prassides, K. Tanigaki and K. Vavekis, *Chem. Commun.*, 1996, 2465.
33 K. Prassides, J. Tomkinson, C. Christides, M. J. Rosseinsky and D. W. Murphy, *Nature*, 1991, **354**, 462.
34 J.-L. Sauvajol, E. Anglaret, R. Aznar, D. Bormann and B. Hennion, *Solid State Commun.*, 1997, **104**, 387.
35 C. M. Brown, D. Phil. Thesis, University of Sussex, 1999.
36 L. Cristofolini, K. Vavekis, K. Prassides, A. J. Dianoux, M. Kosaka, I. Hirosawa and K. Tanigaki, *Physica B*, 1996, **226**, 41.